Ore Geology Reviews 164 (2024) 105846

Contents lists available at ScienceDirect

Ore Geology Reviews

journal homepage: www.elsevier.com/locate/oregeorev

Ore genesis of the Tieshajie Cu deposit: Implications for Cu mineralization in the Qin-Hang Metallogenic Belt, South China

Chengyao Jiang [a], Peng Liu [b,c,*], Sarah A. Gleeson [c,d], Zhian Bao [b], Chao Li [e], Ryan Mathur [f], Yongpeng Ouyang [g], Nan Lv [b], Jingwen Mao [a,h], Honglin Yuan [b]

[a] School of Earth Sciences and Resources, Chang'an University, Xi'an 710054, China
[b] State Key Laboratory of Continental Dynamics, Department of Geology, Northwest University, Xi'an 710069, China
[c] GFZ German Research Centre for Geosciences, Potsdam 14473, Germany
[d] Institute of Geological Sciences, Freie Universität Berlin, Berlin 14463, Germany
[e] National Research Center for Geoanalysis, Chinese Academy of Geological Sciences, Beijing 100037, China
[f] Department of Geology, Juniata College, Huntingdon, PA 16652, USA
[g] The Tenth Geological Brigade of Jiangxi Geological Bureau, Yingtan 335001, China
[h] MNR Key Laboratory for Exploration Theory & Technology of Critical Mineral Resources, China University of Geosciences, Beijing 100083, China

ARTICLE INFO

Keywords:
Titanite
In-situ S-Cu isotope
Re-Os isotope
Tieshajie Cu deposit
South China

ABSTRACT

The Tieshajie Cu deposit, located in the northeastern part of the Qin-Hang Metallogenic Belt (QHMB), South China, has long been regarded as a representative Meso-Neoproterozoic volcanogenic massive sulfide (VMS) deposit. Here we present a hydrothermal titanite U-Pb age, Re-Os and *in-situ* S-Cu isotope data for chalcopyrite to constrain the timing and ore genesis of the Tieshajie deposit. Laser ablation-inductively coupled plasma-mass spectrometry (LA-ICP-MS) U-Pb dating of titanite from the disseminated Cu ore yielded a weighted mean $^{206}Pb/^{238}U$ age of 160.1 ± 4.4 Ma. Chalcopyrite from different ore types has low $^{187}Os/^{188}Os$ (0.85–3.60) and $^{187}Re/^{188}Os$ (46.1–614.0) ratios, combined with initial $^{187}Os/^{188}Os$ (0.74–2.00), excluding a mantle source. A Re-Os isochron age (188 ± 30 Ma) for five chalcopyrite samples is consistent with the titanite U-Pb age within errors. Moreover, the variations in Cu isotope compositions ($\delta^{65}Cu$: −1.13 to +0.12 ‰) and $\delta^{34}S$ values (+3.8 to +7.7 ‰) of chalcopyrite are inconsistent with those reported from the ancient VMS deposits in previous studies. Therefore, our results are indicative of a Late Jurassic magmatic-hydrothermal origin instead of a VMS origin for the Tieshajie deposit. In combination with previous studies, we propose that the Tieshajie Cu deposit belongs to the distal part of the Mid-Late Jurassic (170–150 Ma) porphyry-skarn Cu mineralization event in the QHMB, likely triggered by the subduction of the Paleo-Pacific plate during the Late Mesozoic. This study also has new insights into the genesis of Cu mineralization in the QHMB and further provides implications for future exploration.

1. Introduction

The collision and amalgamation of the Yangtze Craton and Cathaysia Block during the Neoproterozoic in South China led to the formation of the Qin-Hang suture zone (Mao et al., 2011; Shu, 2012). Following the amalgamation, the Qin-Hang Metallogenic Belt (QHMB), a significant zone of porphyry-skarn Cu-polymetallic mineralization, was developed along the suture zone during the Mid-Late Jurassic. The QHMB includes numerous Cu-polymetallic deposits, e.g., the Dexing, Yinshan, Yongping, Yuanzhuding, Baoshan, and Qibaoshan deposits (Mao et al., 2013). Recently, there has been a consensus that Late Mesozoic deposits and associated magmatism in the QHMB link to the regional geodynamics, but there are divergent perspectives regarding the nature of the geodynamic controls. For instance, Mao et al. (2021) proposed that these Cu-polymetallic deposits were related to the mantle and lower-crustal melts from the subduction-metasomatized lithosphere, triggered by a low-angle subduction of the Paleo-Pacific plate beneath the South China during the Middle-Late Jurassic. In contrast, Zhou et al. (2017) suggested that these porphyry Cu deposits were associated with the partial melting of the lower crust induced by the continental crustal extension and thinning, and upwelling of the asthenospheric mantle. Moreover, there are several deposits in the northeastern part of the QHMB (e.g.,

* Corresponding author at: State Key Laboratory of Continental Dynamics, Department of Geology, Northwest University, Xi'an 710069, China.
E-mail address: pengliu@nwu.edu.cn (P. Liu).

https://doi.org/10.1016/j.oregeorev.2023.105846
Received 15 June 2023; Received in revised form 26 November 2023; Accepted 20 December 2023
Available online 26 December 2023

Pingshui and Tieshajie) which have long been regarded to be Neoproterozoic volcanic-associated massive sulfide (VMS) deposits and have been interpreted as reflecting the existence of metal-rich juvenile crust in the Neoproterozic (Wang et al., 2018; Chen et al., 2014). It has been suggested, therefore, that the coeval formation of metal-rich juvenile crust with these Neoproterozoic VMS deposits, which was subsequently partially melted in the Mesozoic, could be a "vital step" for the formation of the regional Mesozoic extensive development of porphyry copper–gold mineralization (Ni and Wang, 2017). However, although previous investigations have primarily concentrated on deposit geology and metamorphic petrology in these VMS deposits, the mineralization has not been dated, and therefore, their genesis remains equivocal.

The Tieshajie Cu deposit (5.2 Mt ores with a mean Cu grade of 1.07 wt%; Wang et al., 2018), is a stratiform-like sulfide deposit hosted by strongly metamorphosed and deformed Meso-Neoproterozoic strata. It has long been proposed that the Tieshajie deposit exhibits characteristics typical of VMS deposits, such as lenticular and stratiform-like orebodies that are semiconformable hosted in the Meso-Neoproterozoic marine volcanic strata (Ye, 1987; He et al., 2008; Wang et al., 2018). These volcanic host rocks have been accurately dated using the LA-ICP-MS zircon U-Pb method, revealing ages ranging from 1172 to 980 Ma (He et al., 2008; Ni and Wang, 2017; Wang et al., 2018; Gao et al., 2013; Zhu, 2017). However, the lack of direct dating of the mineralization means the nature and genesis of the deposit remain ambiguous, and this extends to a more precise comprehension of the metal source. Here, we present a hydrothermal titanite LA-ICP-MS U-Pb age and constrain the timing of the Tieshajie Cu mineralization. We also present Re-Os isotope and *in-situ* S-Cu data of chalcopyrite to constrain the source of the metals and sulfur within the system. Our new results suggest that the Tieshajie deposit has a magmatic-hydrothermal origin, and belongs to the distal part of the Mid-Late Jurassic (170–150 Ma) porphyry-skarn Cu metallogenic event in the QHMB.

2. Geological setting

2.1. Regional geology

The convergence between the Yangtze Craton and Cathaysia Block occurred in the Neoproterozoic (Zhao and Cawood, 2012) (Fig. 1). It resulted in tectono-magmatic and metamorphic events in South China, from 910 to 720 Ma and the formation of volcano-sedimentary complexes such as the Pingshui, Shuangxiwu, Chencai, Zhoutan, Shuangqiaoshan, and Tieshajie Groups (Shu, 2006; Charvet et al., 2010).

The assembly of the Cathaysia Block and Yangtze Craton during the Neoproterozoic era resulted in the development of the Qin-Hang suture zone in South China. (Fig. 1; Chen and Jahn, 1998). In the northeastern part of the Qin-Hang suture zone, the exposed strata primarily comprise Neoproterozoic Shuangqiaoshan Group, characterized by low-grade metamorphic sedimentary rocks and mafic volcanic formations. This unit was overlain or intruded by Middle Jurassic volcanic-subvolcanic rocks. In the late Mesozoic, Paleo-Pacific plate beneath the South China block subducted northwest resulted in the formation of Mid-Late Jurassic calc-alkaline granitoids with comparatively high $\varepsilon_{Nd(t)}$ values and younger model ages (T_{2DM}) in South China (Gilder et al., 1996). Moreover, a sequence of Mid-Late Jurassic (170–150 Ma) magmatic-hydrothermal Cu-Au-Ag-Pb-Zn polymetallic deposits are dispersed along the Qin-Hang zone and its adjacent regions (referred to as the QHMB) (Mao et al., 2011), including the Jiande skarn Cu, Tongcun porphyry Mo-Cu, Dexing porphyry Cu, Yinshan epithermal Cu-Ag-Pb-Zn, Tongshan skarn Cu, Chuankeng skarn Cu, Longtougang skarn Cu-Zn, Yongping skarn Cu, Baoshan porphyry-skarn Cu-Mo, Yuanzhuding porphyry Cu-Mo, Qibaoshan porphyry Cu, Dabaoshan skarn Cu-Mo-Pb-

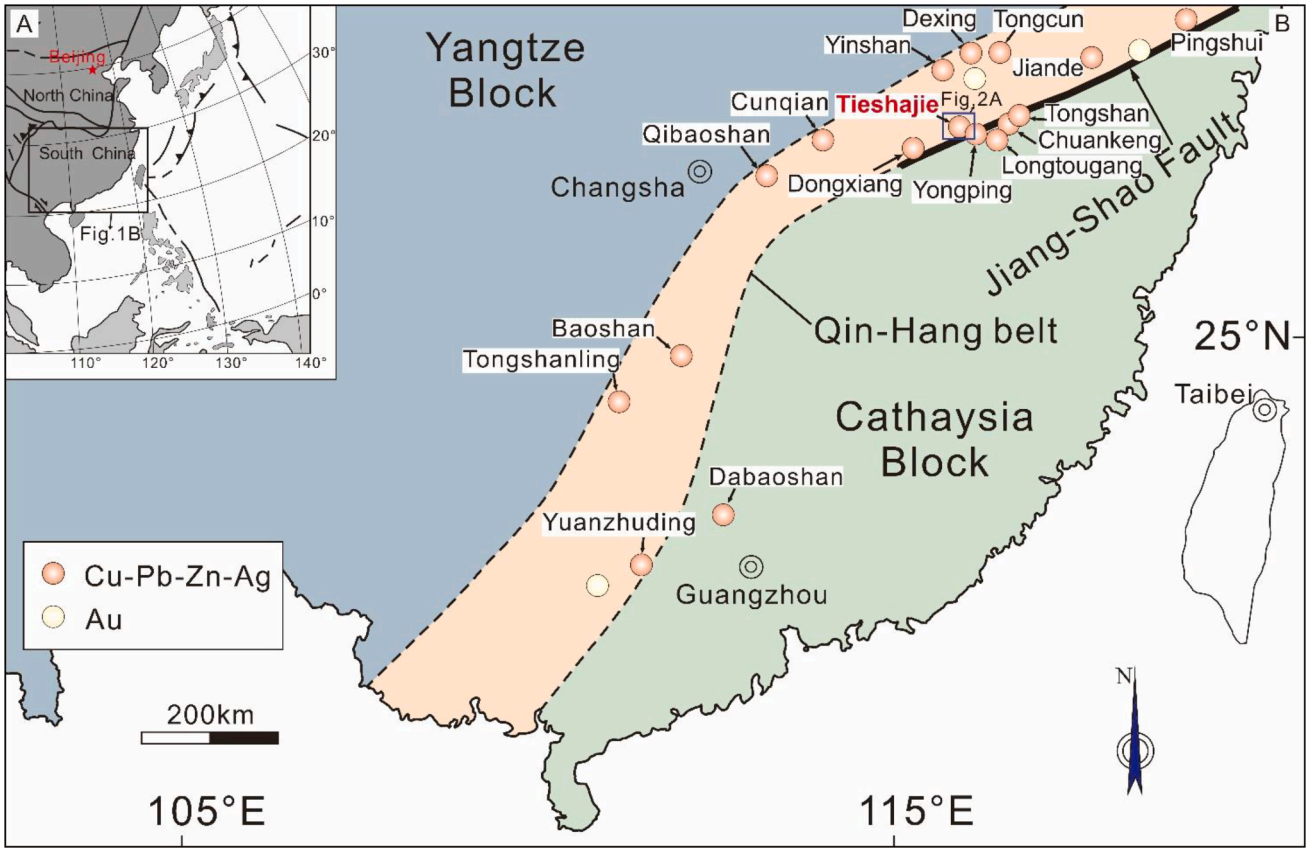

Fig.1. A. Schematic map of tectonic domains of China. B. Spatial distribution of the major mineral deposits in the Qin-Hang metallogenic belt in South China (modified after Ni et al., 2015; Mao et al., 2013).

Zn-Ag and Dongxiang hydrothermal Cu deposits (Mao et al., 2013).

2.2. Deposit geology

The Tieshajie deposit is situated in the northeastern domain of the QHMB, northeastern Jiangxi Province (Fig. 1). The strata exposed in the mine area include the Meso-Neoproterozoic Tieshajie Group and Lower-Middle Jurassic Linshan Group (Fig. 2A, B). The Tieshajie Group occurs in the central part of the area. It is a marine 1081-m-thick extrusive-sedimentary rock sequence, including phyllite, slate, silty sandstone, greywacke, basalts, spilite, quartz keratophyre, limestone, tuff, rhyolite, and marble rocks. The initial lithostratigraphic sequence of the Tieshajie Group has been disintegrated, with now the rhyolites, basalts, and marbles are intercalated (Cheng et al., 1991). Zircon U-Pb age constrains formation time of the Tieshajie Group, including a quartz keratophyre (1201–1091 Ma; He et al., 2008), basalts (1012 ± 4 Ma; Wang et al., 2018), rhyolite (1132–1172 Ma; Gao et al., 2013), spilite (1153–980 Ma; Luo, 2010) and tuff (1109 ± 3 Ma; Zhu, 2017). The Tieshajie Group is unconformably overlain by the Jurassic Linshan Group in the south of the area, which predominantly consists of conglomerate, sandstone, and siltstone. The intrusive rocks primarily consist of granite porphyry and quartz porphyry dikes, emplaced in the Meso-Neoproterozoic Tieshajie

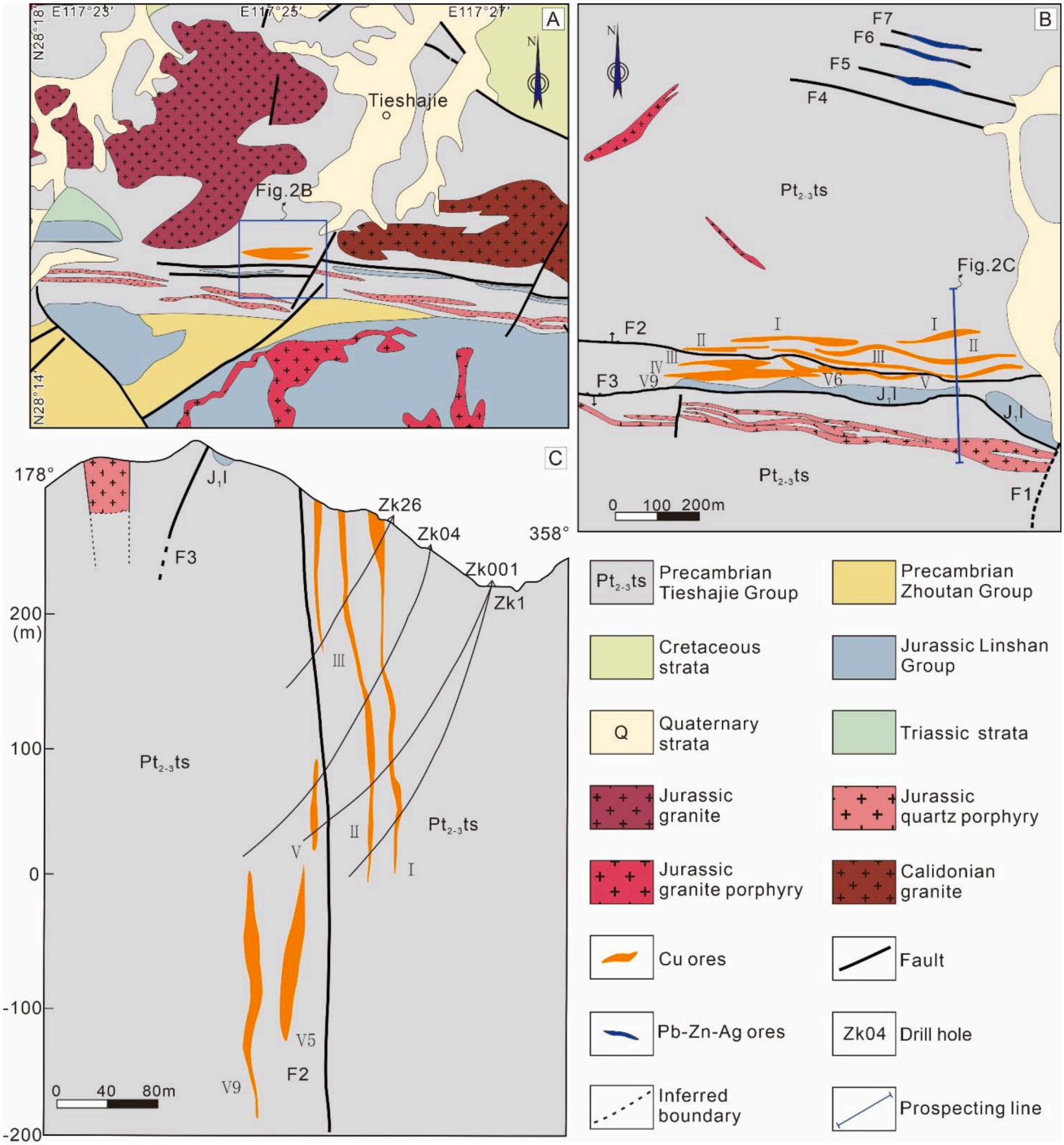

Fig. 2. A. Geologic map of the Tieshajie area (modified after Wang et al., 2018). B. Geological map of the Tieshajie deposit (modified after Zhu, 2017). Orebodies V, V_6 and V_9 are projected to the surface. C. Cross section of the Tieshajie Cu deposit (modified after Wang et al., 2018).

Group. The granite porphyry occurs in the central and northwestern parts of the mine area. The E-W striking quartz porphyry dikes are mostly exposed adjacent to the southern part of the mine area, and vary in width from 15 to 20 m and continue along strike for about 800 m, and have a whole rock K-Ar age of 158.1 Ma (Luo, 2010). The predominant structures in the area are E-W and NNE-SSW–striking faults which were formed along the weak zones of the Tieshajie Group (Wang et al., 2018), for example, the E-W–striking Caopinwu-Zhangjialong faults, which strike 180 to 200° and dip 70 to 90°.

In the mine area, there are twenty-six lenticular, and stratiform-like Cu orebodies that extend from 226 m (surface) to −220 m in elevation. These orebodies are mostly contained inside the interlayered fracture zones and are parallel to each other, with a distance of generally 15–30 m between adjacent orebodies (Fig. 2C). The orebodies dip north at 80 to 85°, range in average thickness from 3.5 to 5 m and have an average strike length of about 400 m.

Based on previous studies and field investigation, we have identified three-style of ores in the Tieshajie deposit: 1) massive ores (Fig. 3A, B), 2) disseminated ores (Fig. 3C, D), and 3) veinlet ores (Fig. 3E, F). Style 1 mineralization is primarily observed in the central part of the orebodies. The ore minerals consist of chalcopyrite, pyrite, and arsenopyrite with minor galena and sphalerite. The major gangue minerals are quartz, actinolite, K-feldspar, and sericite with minor calcite, and titanite. Chalcopyrite is the major ore mineral in the style 1 mineralization, coexisting with anhedral pyrite, euhedral fine-grained arsenopyrite, galena, and sphalerite. The sulfides are intergrown with subhedral quartz, actinolite, and K-feldspar, as well as fine-grained sericite, calcite, and titanite, forming massive ores (Fig. 4A). In addition, framboidal and gelatinous pyrite have been documented in previous publications in the massive ores (Xu, 1992; Wang et al., 2018; Ni and Wang, 2017). Style 2 mineralization predominantly occurs in the host volcanic rock. The ore minerals primarily consist of chalcopyrite, pyrite, and sphalerite, while gangue minerals are dominated by quartz, actinolite, calcite, sericite, and chlorite with minor K-feldspar. Chalcopyrite, pyrite, and sphalerite occur as subhedral to anhedral grains in disseminated ores, while quartz and actinolite occur as subhedral grains together with anhedral fine-grained calcite, sericite, and chlorite forming aggregates (Fig. 4B–D). Style 3 mineralization is primarily developed in the margin of orebodies. Ore minerals primarily comprise of chalcopyrite, pyrite, arsenopyrite, and sphalerite, while the major gangue minerals contain quartz, sericite, calcite, and chlorite. Chalcopyrite, pyrite, arsenopyrite are subhedral to anhedral in quartz-calcite veinlets; sericite and chlorite occur as euhedral to subhedral grains in the veinlets of sulfide-quartz-calcite (Fig. 4E–I).

Ore-related hydrothermal alteration in the Tieshajie deposit includes silicification, actinolitization, potassic alteration, sericitization, and chloritization. Silicification is developed, and is represented as veins or disseminations in all the three-style of ores. Actinolitization mainly occurs as radial and needle-like actinolite in massive and disseminated ore (Fig. 4B). Potassic alteration is commonly associated with massive mineralization, and is in an assemblage with chalcopyrite (Fig. 3G–H). Sericite and chlorite predominantly occur as clusters in disseminated

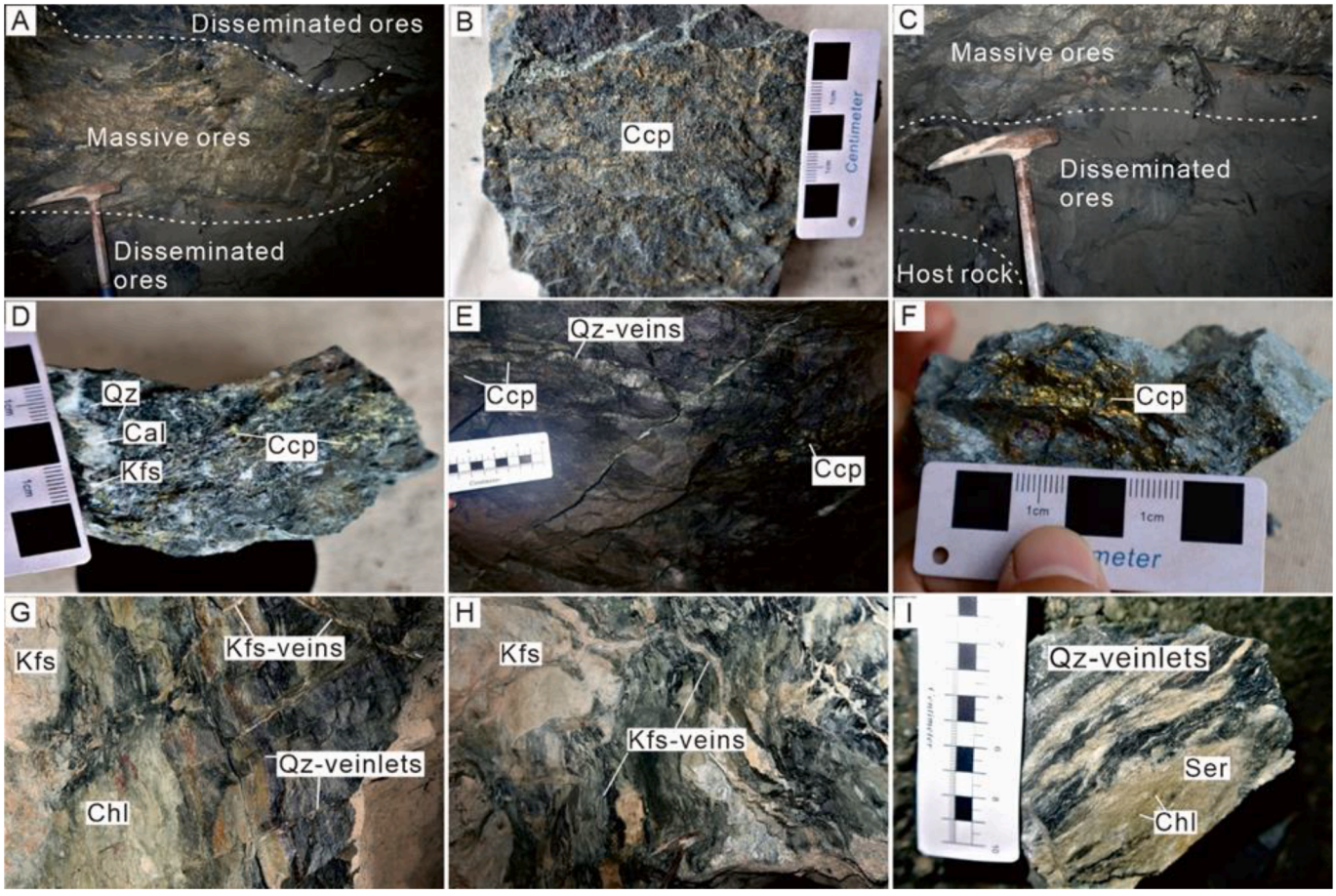

Fig. 3. Photographs of the ores at the Tieshajie deposit. A. Photograph of the massive sulfide ores. B. Photograph of the massive sulfide ore. C. Photograph of the massive and disseminated sulfide ores, and host rock. D. Photograph of the carbonatization, silicification and potassic alteration in the disseminated ore. E. Photograph of the veins of chalcopyrite-quartz in the metamorphic volcanic-sedimentary rocks. F. Photograph of the veinlet sulfide ore. G. Photograph of the potassic alteration and chloritization. H. Photograph of the intense potassic alteration. I. Photograph of the chloritization and sericitization in the rhyolite. Abbreviations: Cal = calcite, Ccp = chalcopyrite, Chl = chlorite, Kfs = K-feldspar, Qz = quartz, Ser = sericite.

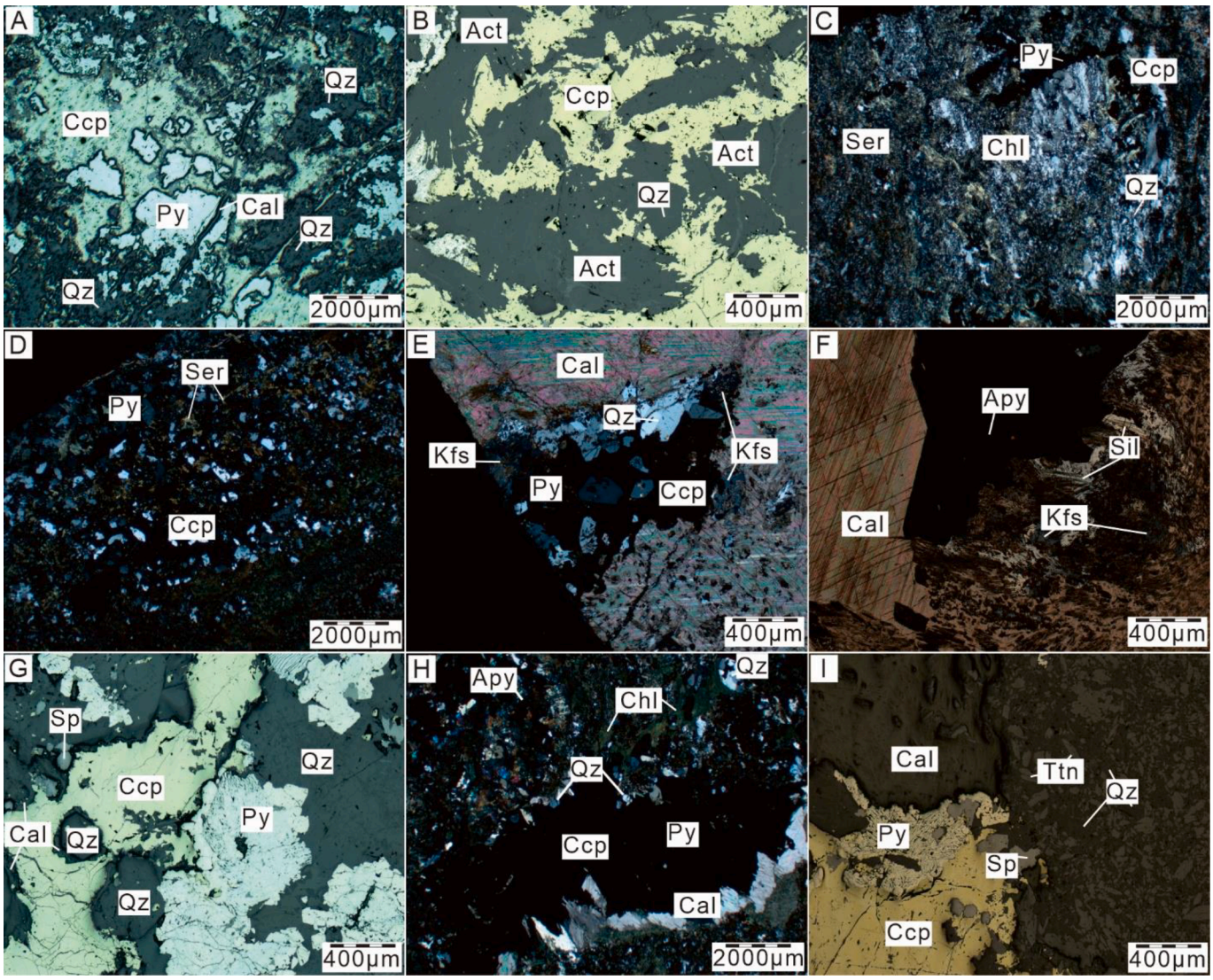

Fig. 4. Photomicrographs of the ores at the Tieshajie Cu deposit. A. Massive ore under plane-polarized reflected light (PPRL). B. Actinolitization and disseminated ore (PPRL). C. Disseminated ore under cross-polarized light (XPL). D. Silicification and sericitization (XPL). E. Calcite-quartz-sulfide vein ore (XPL). F. Potassic alteration and carbonatization under plane-polarized transmitted light. G. Quartz-sulfide vein ore (PPRL). H. Chloritization and sulfide vein ore (XPL). I. Calcite-sulfide vein and hydrothermal titanite (PPRL). Abbreviations: Act = actinolite, Apy = arsenopyrite, Py = pyrite, Sil = sillimanite, Sp = sphalerite, Ttn = titanite.

and veinlet ores.

3. Sampling and analytical methods

We took 10 representative samples from the V9 orebody (underground −200 m). Field investigation, petrographic and mineragraphic studies have been conducted, and then we focused on samples from different ore types (see details below) suitable for geochronological and S-Cu isotope studies. The titanite samples were collected from disseminated ore (TSJ-05) and were used for trace elemental analyses and *in-situ* LA-ICP-MS U–Pb dating. Sample TSJ-05 consists of quartz (35 vol%), chlorite (30 vol%), chalcopyrite (25 vol%), pyrite (5 vol%), titanite (4 vol%), and arsenopyrite (1 vol%), with minor amounts of calcite. Carefully prepared polished thin sections were subjected to thorough examination using both transmitted and reflected light microscopy to discern and analyze the intricate mineral paragenetic relationships. In particular, detailed investigations were conducted utilizing back-scattered electron (BSE) image to discern titanite morphology and internal structures. The findings demonstrate that the titanite grains are intergrown with Cu sulfides, exhibiting a size range primarily between 0.1 and 1.5 mm (euhedral to subhedral), lacking any oscillatory zoning (Fig. 5). Titanite grains were scrutinized utilizing photomicrographs and BSE images for imperfections such as fractures, inclusions, or alterations, and suitable targets were recorded in a series of high-definition images, which were subsequently utilized for trace-element and U-Pb dating analyses.

Chalcopyrite samples for *in-situ* S-Cu isotope analyses were collected from four representative ore samples (TSJ-07, 08, 11, and 12) to obtain isotope variations from the different ore types. Sample TSJ-07 represents veinlet ores, and was collected from the margin of ore lenses. Samples of massive ore (TSJ-08 and 11) and disseminated ore (TSJ-12) were collected from the core of ore lenses. In addition, ten chalcopyrite samples for Re-Os isotope analyses were obtained from the veinlet ores (TSJ-06, 07), massive ores (TSJ-03, 08, 09, 11, 13), and disseminated ores (TSJ-01, 04, 05, 10, 12). The chalcopyrite samples for Re-Os isotopic analysis were extracted utilizing conventional mineral separation techniques, yielding a quantity of approximately 220 to 2000 mg of separated chalcopyrite.

The analytical methods of Re-Os and *in-situ* S isotopes of chalcopyrite are presented in the Appendix.

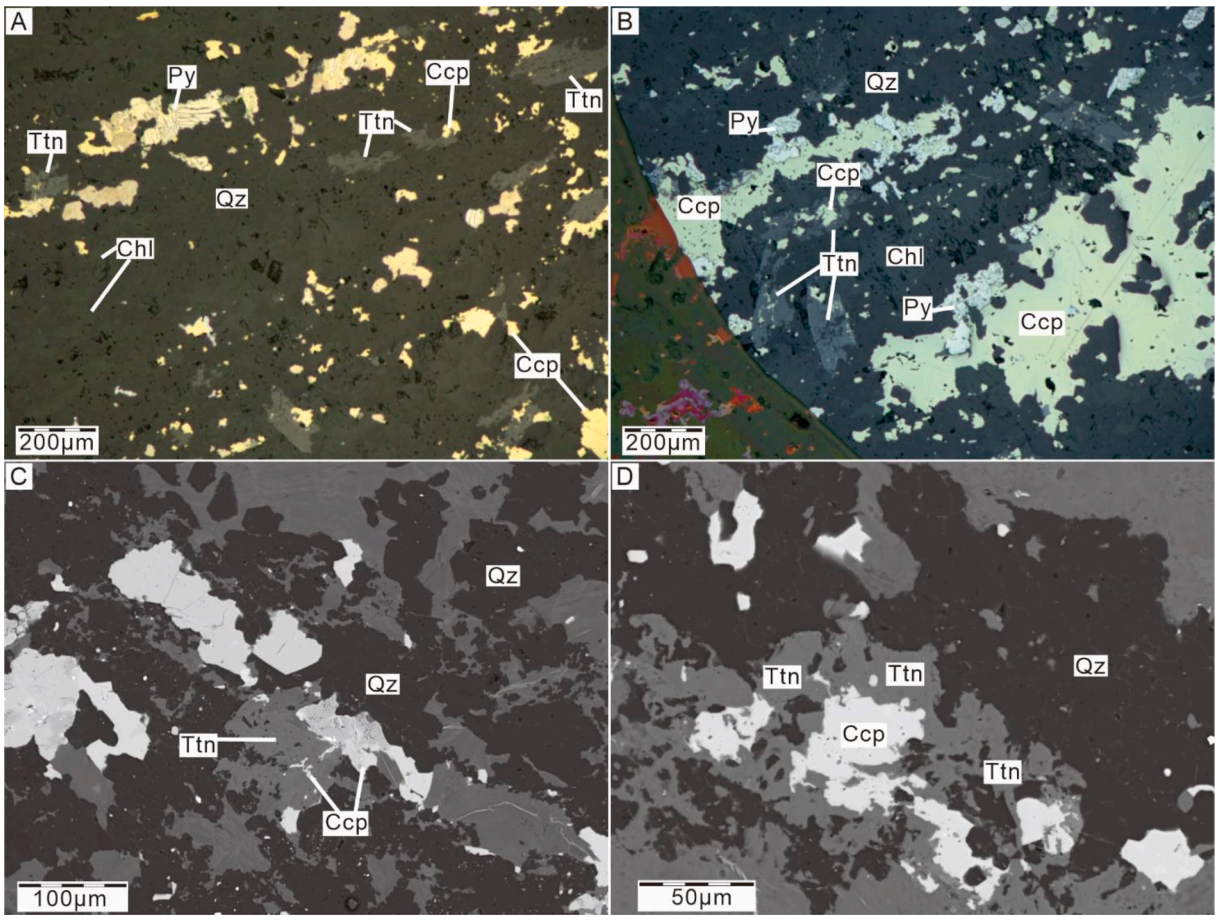

Fig. 5. Photomicrographs of titanite in the Tieshajie Cu ores. A. The coexistence of titanite and chalcopyrite (PPRL). B. The coexistence of titanite, pyrite, and chalcopyrite (PPRL). C and D. Back-scattered electron (BSE) image of the coexisting titanite, quartz, and chalcopyrite.

3.1. Trace element of titanite

All the *in-situ* trace elements analysis of titanite were analyzed at the State Key Laboratory of Continental Dynamics, Northwest University, China. *In-situ* mineral trace element was performed on thin sections using an Agilent 7900 ICP–MS coupled with RESOlution M-50 193-nm ArF Excimer Laser Ablation system. Helium and argon gases were mixed using a T-connector prior to their introduction into the ICP. Laser ablation spot sizes were set to a width of 37 μm for trace element analysis of minerals. For multiple-standard calibration, standard materials including SRM610, BIR-1G, and BCR-2G were utilized. The internal calibration standard was ^{29}Si, and NIST 610 functioned as the external calibration standard. To achieve reliable trace element analysis, offline signal selection techniques were employed using the Excel-based tool ICPMSDataCal. These techniques involved synthesizing background and analyzed signals, correcting for temporal drift, and performing quantitative calibration (Liu et al., 2008).

3.2. In-situ LA–ICP–MS U–Pb titanite dating

In-situ U-Pb isotopes analyses of titanite from the sample disseminated ores were carried out at Yanduzhongshi Geological Analysis Laboratories in China, using an Analytikjena M90 quadrupole ICPMS equipped with a 193 nm NWR193 Ar–F excimer laser. The laser diameter of 20 μm was applied to each spot analysis, with a 7 Hz repetition rate. The dwell time for the isotopes was as follows: 10 ms for ^{29}Si, ^{43}Ca, ^{232}Th and ^{238}U, 15 ms for ^{204}Pb, ^{206}Pb and ^{208}Pb, and 30 ms for ^{207}Pb. Each measurement involved a 20-second background acquisition, succeeded by a 60-second data acquisition from the sample. Subsequently, a 60-second period was designated for the purpose of purging the sample cell and plumbing lines. The matrix-matched BLR-1 titanite, with a known age of 1041.1 ± 0.4 Ma (Aleinikoff et al., 2007), was utilized as a calibration material to account for mass discrimination and U-Pb isotope fractionation. As a quality control material, the OLT-1 titanite (1015 ± 2 Ma; Kennedy et al., 2010) was approved for use in the method. The ICPMSDatCal 10.2 software was used for data reduction, which involved selective signal integration and converting integrated signals to element concentrations (Liu et al., 2010).

3.3. Fs-LA-MC-ICP-MS in-situ Cu isotope of chalcopyrite

In-situ Cu isotope analyses of chalcopyrite were done at the State Key Laboratory of Continental Dynamics, Northwest University, Xi'an, using a Neptune Plus™ MC-ICP-MS combined with an NWR Femto^{UC} dual-wave femtosecond laser ablation (ESI, USA) at SKLCD. The sophisticated line-scan mode was used for all measurements, which had parameters including a diameter of 20 μm, an 8 Hz laser repetition rate, a 1 μm s^{-1} scan speed, and a 0.5 J cm^{-2} laser energy density. Each individual measurement extended over a duration of 142.4 s, encompassing significant stages such as a meticulous 30-second background measurement, followed by a precise 52.4-second data acquisition phase. Subsequently, a thorough 60-second washout period was employed to ensure the removal of any residual effects. The experimental lines utilized for these analyses exhibited an approximate length of 52.4 μm, facilitating a comprehensive assessment of the sample. During the analysis, instrument drift and mass bias were corrected utilizing the standard-sample bracketing (SSB) method. Chalcopyrite was measured using the external standard TC1725 (Bao et al., 2021a, δ^{65}Cu = −0.06

‰), and the accuracy of the measurement was assessed using an in-house standard (CPY-1, chalcopyrite, $\delta^{65}Cu$ = +0.06 ‰, Bao et al., 2021b) as a control-quality standard. Cu isotope data are represented as $\delta^{65}Cu$ values relative to the NIST SRM 976 standard in delta notation: $\delta^{65}Cu_{NIST976} = [(^{65}Cu/^{63}Cu_{sample})/(^{65}Cu/^{63}Cu)_{TC1725}-1] \times 1000 + \delta^{65}Cu_{NIST976(TC1725)}$. The detailed *in-situ* Cu isotope-analysis procedures are elaborated in Bao et al., (2021b) and Lv et al. (2022).

4. Results

4.1. Trace elements of titanite

The titanite grains intergrown with chalcopyrite contain 6–82 ppm U and 2–21 ppm Th, with low Th/U ratios varying between 0.14 and 0.53. Moreover, the titanite grains exhibit relatively low concentrations of REE (121–3200 ppm, mean = 692 ppm) and are are characterized by a depletion in LREE, with LREE/HREE ratios ranging between 0.16 and 1.29 (mean = 0.76) (Appendix Table A1). On chondrite-normalized REE diagrams (Fig. 6A), the titanite displays positive Eu anomalies (Eu/Eu* = 0.80–4.68; mean = 2.49) and weakly positive Ce anomalies (Ce/Ce* = 0.92–1.30; mean = 1.19) (Fig. 6A), with $(La/Yb)_N$ ratios varying between 0.004 and 0.122.

4.2. In-situ U-Pb age of titanite

Eighteen spots were examined on eighteen titanite grains from sample TSJ-5. The U-Pb isotope data acquired from these titanite samples are depicted on a Tera-Wasserburg diagram, exhibiting a well-defined linear array. This linear array yields a lower intercept age of 161.4 ± 6.0 Ma (MSWD = 1.6) (Fig. 6B; Appendix Table A2). The weighted average $^{206}Pb/^{238}U$ age after ^{207}Pb-correction is 160.1 ± 4.4 Ma (MSWD = 1.2) (Fig. 6B), consistent with the lower-intercept age within error.

4.3. In-situ sulfur and copper isotopes

The chalcopyrite from ore samples has a limited range of $\delta^{34}S$ values, varying between +3.8 and +7.7 ‰ (mean = +5.9 ‰) (Fig. 7; Appendix Table A3). The $\delta^{34}S$ values from chalcopyrite in the massive ore (+5.0 to +7.4 ‰, sample TSJ-08, 11) are relatively homogeneous compared to the veinlet ores (+3.8 to +7.7 ‰, sample TSJ-07). The chalcopyrite in the disseminated ore yields $\delta^{34}S$ values from +5.0 to +5.8 ‰.

The chalcopyrite from ore samples for Cu isotope analysis is from the central part of the Tieshajie deposit, with significant $\delta^{65}Cu$ variation between −1.13 and +0.15 ‰ (Fig. 8A, B; Table 1). The chalcopyrite in the massive ore (sample TSJ-11) has $\delta^{65}Cu$ values varying between +0.09 and +0.15 ‰ (mean = +0.12 ‰, n = 13). The chalcopyrite in the veinlet ore (sample TSJ-07) displays lower $\delta^{65}Cu$ values ranging between −1.13 and −0.84 ‰ (mean = −1.03 ‰, n = 11), and the chalcopyrite in the disseminated ore (sample TSJ-12) yields $\delta^{65}Cu$ values varying between −0.01 ‰ and +0.12 ‰ (mean = +0.05 ‰, n = 15) (Fig. 8B).

4.4. Re-Os isotopes of chalcopyrite

Ten analyses of chalcopyrite at Tieshajie contain low total Re (0.2528 to 4.5999 ppb), low ^{187}Os (0.0026 to 0.0211 ppb) and common Os ranging between 0.0085 and 0.0565 ppb. The ranges of ^{187}Os to common Os vary from 0.19 to 0.47, showing significantly low ratios of radiogenic ^{187}Os. The $^{187}Re/^{188}Os$ and $^{187}Os/^{188}Os$ data exhibit scatter around a regression line (Fig. 9A), and yield a low-quality isochron age (253 ± 75 Ma, MSWD = 11644). However, five samples (20TSJ-03, 04, 09, 10, and 11) among the ten samples define a flat-slope isochron with a relatively high-quality age of 188 ± 30 Ma (MSWD = 183) (Fig. 9A). A model age for the system cannot be determined because of the particularly low radiogenic ^{187}Os and low $^{187}Re/^{188}Os$ ratios ranging from 46.1 to 614.0 (Table 2).

5. Discussion

5.1. The timing of the Tieshajie Cu mineralization

Zircon U-Pb ages of the Tieshajie Group range from 1201 to 980 Ma (He et al., 2008; Wang et al., 2018; Gao et al., 2013; Luo, 2010; Zhu, 2017), representing the age of the host rock. It was hoped that the Re-Os study conducted here would directly date the mineralization. The Re-Os isotope data from chalcopyrite have extremely low Re concentrations (mostly < 1 ppb), low $^{187}Re/^{188}Os$ ratios (46.1–614.0), slightly radiogenic $^{187}Os/^{188}Os$ values (0.85–3.60), and yield a low-quality isochron age (253 ± 75 Ma, MSWD = 11644) (Table 2; Fig. 9A). This seems likely to be caused by Re loss, leading to low radiogenic $^{187}Os/^{188}Os$ values. Re loss would cause the isochron anticlockwise rotation (raising the slope)

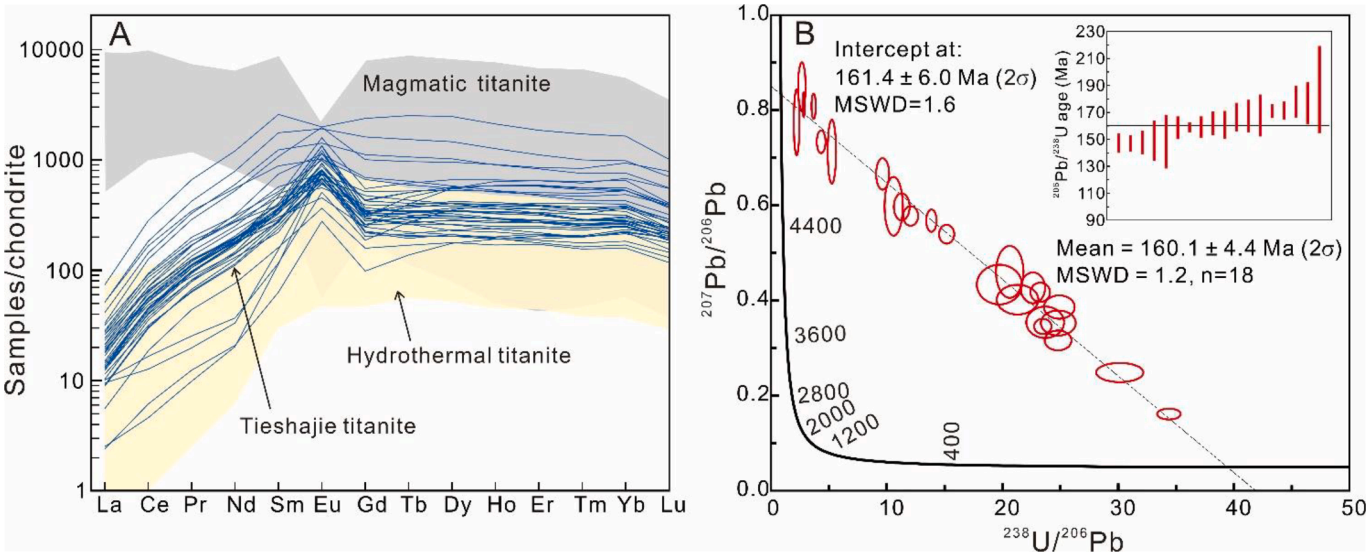

Fig. 6. A. Chondrite-normalized REE patterns of titanite from the Tieshajie deposit. Chondrite REE data from McDonough and Sun (1995). Magmatic and hydrothermal titanite REE compositions from Cao et al. (2015), Li et al. (2010) and Xie et al. (2010). B. Tera-Wasserburg concordia diagrams of the corresponding ^{207}Pb-corrected $^{206}Pb/^{238}U$ ages of titanite in the Tieshajie ores.

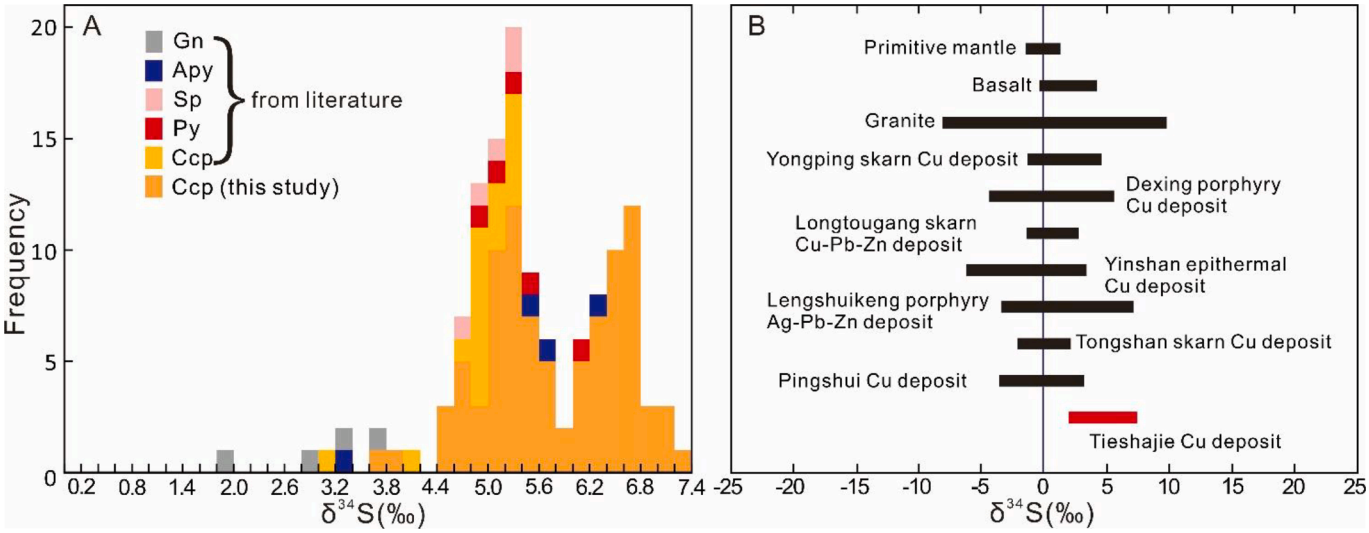

Fig. 7. A. Histograms of $\delta^{34}S$ values of sulfides in the Tieshajie deposit. Data sources from Appendix Table A3. B. Diagram showing variation in $\delta^{34}S$ values of sulfide in the Tieshajie deposit, compared to previous studies on sulfides from the Yanshanian deposits in the northeastern part of QHMB, including the Yongping skarn Cu deposit, the Dexing porphyry Cu deposit, the Longtougang skarn Cu-Pb-Zn deposit, the Yinshan epithermal Cu deposit, the Lengshuikeng Ag-Pb-Zn deposit, the Tongshan skarn Cu deposit, and the Pingshui Cu deposit. Data source from Appendix Table A4. The MORB, basalt, and granite data from Rollinson (1993).

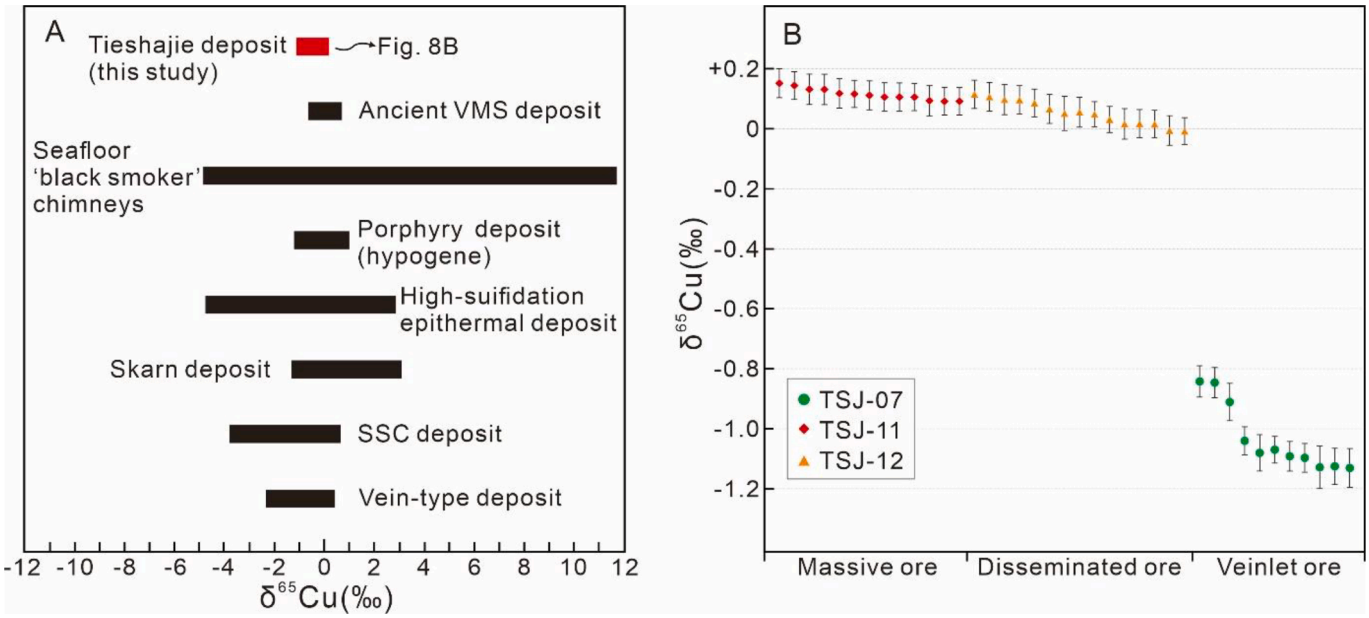

Fig. 8. A. Diagram showing variation in $\delta^{65}Cu$ values of chalcopyrite in the Tieshajie deposit, compared to previous studies on copper-rich minerals from porphyry deposits, high-sulfidation epithermal deposits, skarn deposits, ancient VMS deposits, modern seafloor chimneys, sediment-hosted stratiform copper (SSC) deposits, vein-type deposits. Data source from Appendix Table A6. B. Diagram showing variation in $\delta^{65}Cu$ values of different ores in the Tieshajie deposit.

and drive samples to the lower left of the true isochron (e.g., Mathur et al., 1999; Kemppinen et al., 2018). If the samples with the lowest Re concentrations (0.181–0.847 ppb) are excluded from the calculation, the remaining five samples (20TSJ-03, 04, 09, 10, and 11) with higher Re concentrations (0.455–4.600 ppb) define a relatively flat-slope isochron (Fig. 9A), yielding a relatively high-quality age (188 ± 30 Ma, MSWD = 183). Given that Re loss would define the isochron age older than the true age, the true Re-Os isochron age ought to be younger than 188 Ma.

Hydrothermal titanite U-Pb dating has demonstrated its efficacy as a reliable approach for directly ascertaining the chronology of mineralization events (Jemielita et al., 1990; Frost et al., 2001; Li et al., 2010). Titanite coexisting with chalcopyrite (Fig. 5) is characterized by low concentrations of Th/U (0.15–0.45) and REE (121–3200 ppm, mean = 679 ppm), and displays left-leaning REE patterns with light REE depletion (Fig. 6A), demonstrating a hydrothermal genesis (Aleinikoff et al., 2002; Frost et al., 2001; Li et al., 2010). Moreover, the titanite U-Pb age of 160.1 ± 4.4 Ma is coeval with a K-Ar age of 158.1 Ma obtained for the quartz porphyry in the area (Luo, 2010). Therefore, our new titanite U-Pb age indicates that there is a ca. 160 Ma magmatic-hydrothermal event at Tieshajie which resulted in Cu mineralization.

5.2. Ore-forming material sources

The absence of sulfate minerals in the Tieshajie deposit indicates that the sulfur isotope of H_2S would mostly influence the $\delta^{34}S$ values of sulfide, independent of pH and oxygen fugacity (fO_2) (Ohmoto and Rye, 1979). Therefore, it is reasonable to assume that H_2S was the main sulfur species present in the ore-forming fluid, which means that the $\delta^{34}S$ value

Table 1
In-situ copper isotopic compositions of chalcopyrite from the Tieshajie deposit.

Spot Number	Ore type	Alteration Mineral Assemblages	δ^{65}Cu (‰)	±2σ (‰)
TSJ-12-01	Disseminated ore	Actinolitization sericitization, chloritization, silicification	0.06	0.05
TSJ-12-02			0.02	0.05
TSJ-12-03			0.02	0.05
TSJ-12-04			−0.01	0.05
TSJ-12-05			0.03	0.04
TSJ-12-06			−0.01	0.04
TSJ-12-07			0.05	0.04
TSJ-12-08			0.05	0.06
TSJ-12-09			0.09	0.05
TSJ-12-10			0.10	0.05
TSJ-12-11			0.10	0.05
TSJ-12-12			0.12	0.05
TSJ-12-13			0.02	0.05
TSJ-12-14			0.07	0.05
TSJ-12-15			0.11	0.05
TSJ-11-01	Massive ore	Potassic alteration, actinolitization silicification	0.15	0.05
TSJ-11-02			0.12	0.05
TSJ-11-03			0.12	0.07
TSJ-11-04			0.11	0.04
TSJ-11-05			0.12	0.05
TSJ-11-06			0.09	0.05
TSJ-11-07			0.11	0.05
TSJ-11-08			0.09	0.05
TSJ-11-09			0.11	0.05
TSJ-11-10			0.12	0.05
TSJ-11-11			0.14	0.05
TSJ-11-12			0.13	0.05
TSJ-11-13			0.13	0.05
TSJ-07-01	Veinlet ore	Sericitization, silicification, chloritization	−1.13	0.07
TSJ-07-02			−1.13	0.06
TSJ-07-03			−1.10	0.05
TSJ-07-04			−1.07	0.04
TSJ-07-05			−1.09	0.05
TSJ-07-06			−1.13	0.06
TSJ-07-07			−1.04	0.05
TSJ-07-08			−1.08	0.06
TSJ-07-09			−0.91	0.06
TSJ-07-10			−0.84	0.05
TSJ-07-11			−0.85	0.05

of sulfide represents the bulk sulfur isotopic composition in the fluid of the Tieshajie deposit. In combination with previous S isotope data of sulfide, the sulfide of Tieshajie has δ^{34}S value ranging from +2.0 to +7.7 ‰ (Fig. 7; Appendix Table A3, A4; Luo, 2010; He et al., 2008; Zhu, 2017; Ye, 1987; this study), which is slightly higher than the characteristics of magma sulfur (0 ± 3 ‰; Ohmoto and Goldhaber, 1997). Furthermore, Zheng (2020) reported whole rock δ^{34}S values (+3.2 to +7.2 ‰) for the Tieshajie Group in the region. Thus, the range of δ^{34}S values at Tieshajie suggests a magmatic source with some input of sulfur from the Tieshajie Group.

This is further evidenced by the Pb isotope data presented in previous studies (Luo, 2010; Zhu, 2017). Published Pb isotope data for sulfides at Tieshajie (^{206}Pb/^{204}Pb:17.398–18.489; ^{207}Pb/^{204}Pb: 15.487–15.604; ^{208}Pb/^{204}Pb: 38.237–38.624; Luo, 2010; Zhu, 2017) (Appendix Fig. A1; Appendix Table A5) exhibit similarities to the sulfides observed in the Dexing porphyry Cu deposit in the same region (^{206}Pb/^{204}Pb: 17.889–17.894; ^{207}Pb/^{204}Pb: 15.580–15.583; ^{208}Pb/^{204}Pb: 38.412–38.421; Appendix Fig. A2) (Zhou et al., 2012, 2013). In contrast to an ancient VMS deposit with a homogenous Pb isotopic composition (^{206}Pb/^{204}Pb ratio commonly < 0.1; Franklin et al., 1981, 2005; Thorpe, 1999), the Tieshajie deposit exhibits a large range of ^{206}Pb/^{204}Pb ratios (17.398–18.489). Moreover, there exists an overlap of Pb isotope compositions between the sulfides and plagioclase (^{206}Pb/^{204}Pb: 18.037; ^{207}Pb/^{204}Pb: 15.592; ^{208}Pb/^{204}Pb: 38.340) in the metamorphic sedimentary rocks of the Tieshajie Group (Appendix Fig. A1; Appendix Table A5) (Luo, 2010; Zhu, 2017). The Pb-isotope therefore, also support the interpretation that the ore-forming material was partially derived from the Tieshajie Group.

The chalcopyrite has extremely low Re concentration (mostly <1 ppb), which is inconsistent with sulfides from typical VMS deposits (Fig. 9B). The Re-Os isotope characteristics have been commonly utilized to trace ore metal sources (Morelli et al., 2007; Li et al., 2018; Soares et al., 2021). If the Meso-Neoproterozoic age was utilized to determine the initial ^{187}Os/^{188}Os ratios of chalcopyrite, the ratios have both positive and negative values (−6.84 to 1.04; Table 2), which cannot be explained by a geological scenario. By comparison, the initial ^{187}Os/^{188}Os ratios (0.74 to 2.00; Table 2) calculated at an age of 160 Ma imply a significant crustal derivation (^{187}Os/^{188}Os$_{(\text{mantle-derived magma})}$≈ 0.12, ^{187}Os/^{188}Os$_{(\text{upper crust})}$ = 1.69; Shirey and Walker, 1998; Esser and Turekian, 1993). In general, chalcopyrite from ancient VMS deposits

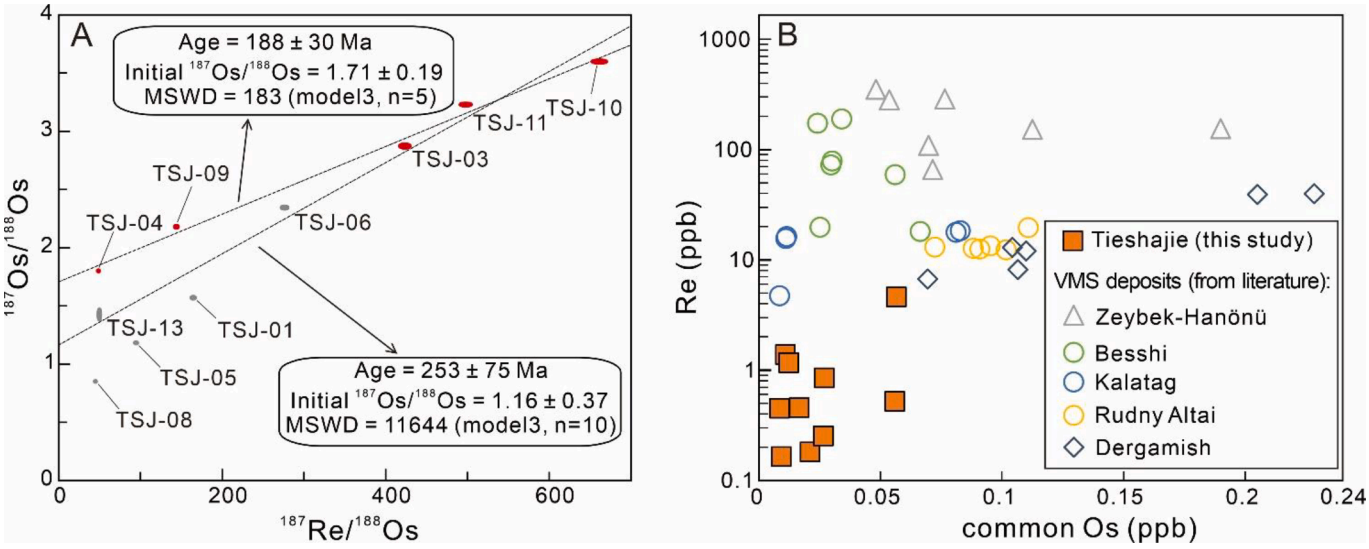

Fig. 9. A. Re-Os isochron diagram of chalcopyrite from the Tieshajie deposit. Ten samples yield a low-quality isochron age of 253 ± 75 Ma (MSWD = 11644), whereas five samples (20TSJ-03, 04, 09, 10, and 11) define a flat-slope isochron with an age of 188 ± 30 Ma (MSWD = 183). B. Plot for Re versus common Os in chalcopyrite from the Tieshajie deposit compared with sulfides from VMS deposits associated with basalt (Data from Günay et al., 2019; Wang et al., 2021; Deng et al., 2016; Lobanov et al., 2014; Gannoun et al., 2003).

Table 2
Re-Os isotopic data of chalcopyrite from the Tieshajie deposit.

Sample ID	Weight (g)	Re (ppb)		Common Os (ppb)		^{187}Os (ppb)		^{187}Re/^{188}Os		^{187}Os/^{188}Os		^{187}Os/Common Os	Os_i (160.1 Ma)	Os_i (1012 Ma)
		Re	2σ	Common Os	2σ	^{187}Os	2σ	Ratio	2σ	Ratio	2σ			
20TSJ-01	0.300	0.847	0.006	0.0268	0.0002	0.0055	0.0000	152.7	1.6	1.571	0.005	0.20	1.16	−1.03
20TSJ-03	0.300	4.600	0.034	0.0565	0.0005	0.0211	0.0002	393.1	4.5	2.875	0.011	0.37	1.82	−3.81
20TSJ-04	0.300	0.520	0.004	0.0558	0.0004	0.0131	0.0001	45.0	0.5	1.802	0.004	0.23	1.68	1.04
20TSJ-05	0.600	0.164	0.001	0.0090	0.0001	0.0014	0.0000	87.7	0.9	1.183	0.003	0.15	0.95	−0.31
20TSJ-06	0.603	0.449	0.003	0.0085	0.0001	0.0026	0.0000	256.5	2.7	2.346	0.007	0.30	1.66	−2.02
20TSJ-08	0.300	0.181	0.002	0.0210	0.0002	0.0023	0.0000	41.6	0.5	0.852	0.003	0.11	0.74	0.14
20TSJ-09	0.602	0.455	0.003	0.0165	0.0001	0.0047	0.0000	133.6	1.4	2.182	0.007	0.28	1.82	−0.09
20TSJ-10	0.600	1.380	0.010	0.0109	0.0001	0.0051	0.0000	614.0	6.3	3.600	0.007	0.47	1.96	−6.84
20TSJ-11	0.602	1.168	0.009	0.0122	0.0001	0.0051	0.0000	462.2	4.8	3.231	0.007	0.42	2.00	−4.63
20TSJ-13	0.300	0.253	0.002	0.0265	0.0003	0.0049	0.0001	46.1	0.7	1.427	0.035	0.19	1.30	0.64

Note: the $(^{187}Os/^{188}Os)_i$ can be calculated from the equation: $^{187}Os/^{188}Os = (^{187}Os/^{188}Os)_i + {}^{187}Re/^{188}Os\,(e^{\lambda t} - 1)$, where λ is the ^{187}Re decay constant ($\lambda = 1.666 \times 10^{-11}$ year^{-1}) (Smoliar et al., 1996).

displays a very limited range of δ^{65}Cu values (Fig. 8A) (−0.62 to +0.70 ‰, close to 0 ‰; Housh and Çiftçi, 2008; Mason et al., 2005; Ikehata et al., 2011; Deng et al., 2019), and particularly the $\Delta\delta^{65}$Cu within a single ancient VMS deposit is commonly less than 1‰, which are distinct from the δ^{65}Cu values (−1.13 to +0.12 ‰) at Tieshajie. Furthermore, the negative δ^{65}Cu trend from massive ore to veinlet ore at Tieshajie correlates to a hydrothermal alteration transformation from potassic to phyllic (Fig. 8B; Table 1), likely suggesting that negative Cu isotope fractionation is more readily induced under stronger acidic hydrothermal conditions (Maher et al., 2011; Gregory and Mathur, 2017). In summary, all the observations indicate the magmatic-hydrothermal origin of the Tieshajie Cu deposit, and the ore-forming material is primarily derived from magmatic-hydrothermal fluids, while there is a minor contribution from the host rock via fluid-rock interactions.

5.3. A genetic model for the Tieshajie Cu mineralization

The consistency of the quartz porphyry and hydrothermal titanite ages suggests a link between the granite intrusions and the mineralization. Therefore, we propose that the Tieshajie Cu deposit may belong to the distal part of a Late Jurassic porphyry system. The orebodies are hosted within the Neoproterozoic meta-sedimentary rock of the Tieshajie Group but the mineralization is genetically relevant to the intrusions with an age of ~160 Ma. Following this, at ca. 160 Ma, when the rising magmas were emplaced into the host rock, the fracture zone in the area reactivated and expanded. The magmatic-hydrothermal fluids emanating from intrusions interacted with the host rock to generate hydrothermal alteration and form the Cu orebodies in the fractures. The age of the Tieshajie Cu deposit is coeval with the Mid-Late Jurassic (170–150 Ma) magmatic-hydrothermal metallogenic event in the QHMB (Mao et al., 2011, 2013) (Fig. 10; Appendix Table A7). This event is interpreted to be connected with the subduction of the Paleo-Pacific plate (Mao et al., 2021). Moreover, published Pb isotope data of sulfide at Tieshajie (^{206}Pb/^{204}Pb: 17.40–18.49; ^{207}Pb/^{204}Pb: 15.49–15.60; Luo, 2010; Zhu, 2017) is similar to the Pacific subduction sediments and enriched mantle (Appendix Fig. A1), and is partially overlapping with the Dexing porphyry Cu-related rocks (Appendix Fig. A2). Therefore, we propose that the Tieshajie Cu mineralization is a Late Jurassic magmatic-hydrothermal mineral system, probably induced by the subduction of the Paleo-Pacific plate. As such, the scenario that the Neoproterozoic VMS deposits and the generation of the coeval metal-rich juvenile crust in the QHMB are the "vital step" in the development of the widespread Mesozoic porphyry copper–gold mineralization at a regional scale may need to be reassessed.

6. Conclusions

1. The new titanite U-Pb age of 160.1 ± 4.4 Ma and the chalcopyrite Re-Os dating indicate an epigenetic magmatic-hydrothermal origin instead of a Neoproterozoic VMS origin for the Tieshajie Cu mineralization.
2. The Re-Os and *in-situ* S-Cu isotope compositions of sulfides indicate a significant crustal contribution to the hydrothermal system. Ore-forming material is mainly from magmatic-hydrothermal fluids with minor contributions from the host rocks via fluid-rock interaction.
3. The Tieshajie Cu mineral system is a distal part of the Late Jurassic porphyry-skarn metallogenic event in the QHMB, South China,

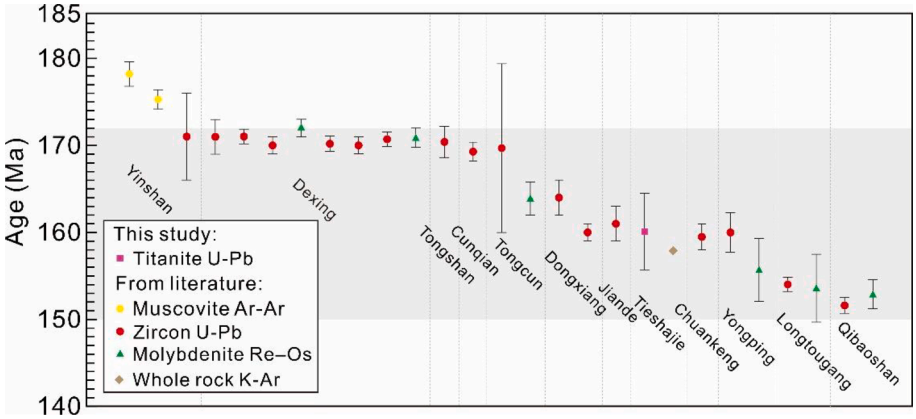

Fig. 10. Compilation of geochronological data for the Yanshanian deposits in the northeastern part of QHMB. Data source from Appendix Table A7.

which was probably triggered by the subduction of the Paleo-Pacific plate.

Declaration of competing interest

The authors declare that they have no known competing financial interests or personal relationships that could have appeared to influence the work reported in this paper.

Data availability

No data was used for the research described in the article.

Acknowledgments

We appreciate the assistance provided by Professor Minwu Liu and Wenlei Song for their valuable technical support with the titanite BSE images. This study was co-funded by the National Natural Science Foundation of China (grants 42130102, 42242201, 42072054, 42173033), the Young Star of Science and Technology Plan Projects in Shaanxi Province, China (Grant 2023KJXX–037), and the Natural Science Basic Research program in Shaanxi Province of China (2022JC-DW5-01). Sarah A. Gleeson is funded by a Helmholtz Recruitment Initiative.

Appendix A. Supplementary data

Supplementary data to this article can be found online at https://doi.org/10.1016/j.oregeorev.2023.105846.

References

Aleinikoff, J.N., Wintsch, R.P., Fanning, C.M., Dorais, M.J., 2002. U-Pb geochronology of zircon and polygenetic titanite from the Glastonbury Complex, Connecticut, USA: an integrated SEM, EMPA, TIMS, and SHRIMP study. Chem. Geol. 188, 125–147.

Aleinikoff, J.N., Wintsch, R.P., Tollo, R.P., Unruh, D.M., Fanning, C.M., Schmitz, M.D., 2007. Ages and origins of rocks of the Killingworth dome, south-central Connecticut: Implications for the tectonic evolution of southern New England. Am. J. Sci. 307, 63–118.

Bao, Z.A., Chen, K.Y., Zong, C.L., Yuan, H.L., 2021a. TC1725: a proposed chalcopyrite reference material for LA-MC-ICP-MS sulfur isotope determination. J. Anal. Atom. Spectrom. 36 (8), 1657–1665.

Bao, Z.A., Lv, N., Chen, K.Y., Luan, Y., Sun, X.H., Zong, C.L., Yuan, H.L., 2021b. A potential new chalcopyrite reference material for LA-MC-ICP-MS copper isotope ratio measurement. Geostand. Geoanal. Res. 45, 401–418.

Cao, M.J., Qin, K.Z., Li, G.M., Evans, N.J., Jin, L.Y., 2015. In situ LA-(MC)-ICP-MS trace element and Nd isotopic compositions and genesis of polygenetic titanite from the Baogutu reduced porphyry Cu deposit, Western Junggar, NW China. Ore Geol. Rev. 65, 940–954.

Charvet, J., Shu, L.S., Faure, M., Choulet, F., Wang, B., Lu, H.F., Breton, N.L., 2010. Structural development of the Lower Paleozoic belt of South China: genesis of an intracontinental orogen. J. Asian Earth Sci. 39, 309–330.

Chen, J.F., Jahn, B.M., 1998. Crustal evolution of southeast China: Nd and Sr isotopic evidence. Tectonophysics 284, 101–133.

Chen, H., Ni, P., Wang, R.C., Wang, G.G., Zhao, K.D., Ding, J.Y., Zhao, C., Cai, Y.T., Xu, Y. F., 2014. A combined fluid inclusion and S-Pb isotope study of the Neoproterozoic Pingshui volcanogenic massive sulfide Cu–Zn deposit, Southeast China. Ore Geol. Rev. 66, 388–402.

Cheng, H., Hu, S.L., Tang, C.H., 1991. New recognition of the isotopic geochronology of the "Tieshajie Group" in the southern part of northeastern Jiangxi. Reg. Geol. China 2, 151–154 in Chinese with English abstract.

Deng, X.H., Wang, J.B., Pirajno, F., Wang, Y.W., Li, Y.C., Li, C., Zhou, L.M., Chen, Y.J., 2016. Re–Os dating of chalcopyrite from selected mineral deposits in the Kalatag district in the eastern Tianshan Orogen, China. Ore Geol. Rev. 77, 72–81.

Deng, X.H., Mathur, R., Li, Y., Mao, Q.G., Wu, Y.S., Yang, L.Y., Chen, X., Xu, J., 2019. Copper and zinc isotope variation of the VMS mineralization in the Kalatag district, eastern Tianshan, NW China. J. Geochem. Explor. 196, 8–19.

Esser, B.K., Turekian, K.K., 1993. The osmium isotopic composition of the continental crust. Geochim. Cosmochim. Acta 57, 3093–3104.

Franklin, J.M., Sangster, D.M., Lydon, J.W., 1981. Volcanic-associated massive sulfide deposits. Econ. Geol. 75th Anniversary Volume, 485–627.

Franklin, J.M., Gibson, H.L., Jonasson, I.R., Galley, A.G., 2005. Volcanogenic massive sulfide deposits. Econ. Geol. 100th Anniversary Volume 523–560.

Frost, B.R., Chamberlain, K.R., Schumacher, J.C., 2001. Sphene (titanite): phase relations and role as a geochronometer. Chem. Geol. 172, 131–148.

Gannoun, A., Tessalina, S., Bourdon, B., Orgeval, J.J., Birck, J.L., Allègre, C.J., 2003. Re–Os isotopic constraints on the genesis and evolution of the Dergamish and Ivanovka Cu (Co, Au) massive sulphide deposits, south Urals, Russia. Chem. Geol. 196, 193–207.

Gao, L.Z., Liu, Y.X., Ding, X.Z., Song, Z.R., Huang, Z.Z., Zhang, C.H., Zhang, H., Shi, Z.G., 2013. Geochronographic dating of the Tieshajie Formation in the Jiangshan-Shaoxing fault zone and its implications. Geol. Bull. China 32, 996–1005 in Chinese with English abstract.

Gilder, S.A., Gill, J., Coe, R.S., Zhao, X.X., Liu, Z.W., Wang, G.X., Yuan, K.R., Liu, W.L., Kuang, G.D., Wu, H.R., 1996. Isotopic and paleomagnetic constraints on the Mesozoic tectonic evolution of South China. J. Geophys. Res. 101, 16137–16154.

Gregory, M.J., Mathur, R., 2017. Understanding copper isotope behavior in the high temperature magmatic-hydrothermal porphyry environment. Geochem. Geophy. Geosy. 18, 4000–4015.

Günay, K., Dönmez, C., Oyan, V., Baran, C., Ciftci, E., Parlak, O., Yıldırım, N., Deng, X.H., Li, C., Yıldırım, E., Özkümüş, S., 2019. Geology, geochemistry and Re-Os geochronology of the Jurassic Zeybek volcanogenic massive sulfide deposit (Central Pontides, Turkey). Ore Geol. Rev. 111, 102994.

He, J.R., Wang, A.G., Rui, X.J., Zeng, Y., Li, C.H., 2008. Middle Proterozoic submarine volcanic exhalative metallogenesis of Tieshajie, Yiyang, Jiangxi Province. Resour. Surv. Environ. 29, 261–269 in Chinese with English abstract.

Housh, T.B., Çiftçi, E., 2008. Cu isotope geochemistry of volcanogenic massive sulphide deposits of the eastern Pontides, Turkey. In: IOP Conference Series: Earth and Environmental Science. IOP Publishing, p. 012025.

Ikehata, K., Notsu, K., Hirata, T., 2011. Copper isotope characteristics of copper-rich minerals from Besshi-type volcanogenic massive sulfide deposits, Japan, determined using a femtosecond LA-MC-ICP-MS. Econ. Geol. 106, 307–316.

Jemielita, R.A., Davis, D.W., Krogh, T.E., 1990. U-Pb evidence for Abitibi gold mineralization postdating greenstone magmatism and metamorphism. Nature 346, 831–834.

Kemppinen, L.I., Kohn, S.C., Parkinson, I.J., Bulanova, G.P., Howell, D., Smith, C.B., 2018. Identification of molybdenite in diamond-hosted sulphide inclusions: Implications for Re–Os radiometric dating. Earth Planet. Sci. Lett. 495, 101–111.

Kennedy, A.K., Kamo, S.L., Nasdala, L., Timms, N.E., 2010. Grenville skarn titanite: potential reference material for SIMS U-Th–Pb analysis. Can. Mineral. 48, 1423–1443.

Li, J.W., Deng, X.D., Zhou, M.F., Liu, Y.S., Zhao, X.F., Guo, J.L., 2010. Laser ablation ICP-MS titanite U-Th–Pb dating of hydrothermal ore deposits: a case study of the Tonglushan Cu–Fe–Au skarn deposit, SE Hubei Province, China. Chem. Geol. 270, 56–67.

Li, Y., Selby, D., Li, X.H., Ottley, C.J., 2018. Multisourced metals enriched by magmatic-hydrothermal fluids in stratabound deposits of the Middle-Lower Yangtze River metallogenic belt, China. Geology 46, 391–394.

Liu, Y.S., Hu, Z.C., Gao, S., Günther, D., Xu, J., Gao, C.G., Chen, H.H., 2008. In situ analysis of major and trace elements of anhydrous minerals by LA-ICP-MS without applying an internal standard. Chem. Geol. 257 (1–2), 34–43.

Liu, Y.S., Gao, S., Hu, Z.C., Gao, C.G., Zong, K.Q., Wang, D.B., 2010. Continental and oceanic crust recycling-induced melt-peridotite interactions in the Trans-North China Orogen: U-Pb dating, Hf isotopes and trace elements in zircons of mantle xenoliths. J. Petrol. 51, 537–571.

Lobanov, K., Yakubchuk, A., Creaser, R.A., 2014. Besshi-type VMS deposits of the Rudny Altai (central Asia). Econ. Geol. 109, 1403–1430.

Luo, P., 2010. Research on Metallogenic regularities and prospecting orientation of Copper polymetal Mineral Resources in the Northern Wuyi region of Jiangxi Province. China University of Geosciences (Beijing), Doctoral Dissertation (in Chinese with English abstract).

Lv, N., Bao, Z.A., Chen, K.Y., Wu, K., Yuan, H.L., 2022. Accurate analysis of Cu isotopes by fs-LA-MC-ICP-MS with non-matrix-matched calibration. Sci. China-Earth Sci. 65, 2005–2017.

Maher, K.C., Jackson, S., Mountain, B., 2011. Experimental evaluation of the fluid–mineral fractionation of Cu isotopes at 250 °C and 300 °C. Chem. Geol. 286, 229–239.

Mao, J.W., Cheng, Y.B., Chen, M.H., Pirajno, F., 2013. Major types and time–space distribution of Mesozoic ore deposits in South China and their geodynamic settings. Miner. Depos. 48, 267–294.

Mao, J.W., Chen, M.H., Yuan, S.D., Guo, C.L., 2011. Geological characteristics of the Qinhang (Shihang) metallogenic belt in South China spatial–temporal distribution of mineral deposits. Acta Geol. Sin. 85, 636–658 in Chinese with English abstract.

Mao, J.W., Zheng, W., Xie, G.Q., Lehmann, B., Goldfarb, R., 2021. Recognition of a Middle-Late Jurassic arc-related porphyry copper belt along the southeast China coast: Geological characteristics and metallogenic implications. Geology 49, 592–596.

Mason, T.F.D., Weiss, D.J., Chapman, J.B., Wilkinson, J.J., Tessalina, S.G., Spiro, B., Horstwood, M., Parrish, R.R., Spratt, J., Coles, B.J., 2005. Zn and Cu isotopic variability in the Alexandrinka volcanic hosted massive sulphide (VHMS) ore deposit, Urals, Russia. Chem. Geol. 221, 170–187.

Mathur, R., Ruiz, J., Tornos, F., 1999. Age and sources of the ore at Tharsis and Rio Tinto, Iberian pyrite belt, from Re-Os isotopes. Miner. Depos. 34, 790–793.

McDonough, W.F., Sun, S.S., 1995. The composition of the Earth. Chem. Geol. 120, 223–253.

Morelli, R., Creaser, R.A., Seltmann, R., Stuart, F.M., Selby, D., Graupner, T., 2007. Age and source constraints for the giant Muruntau gold deposit, Uzbekistan, from coupled Re-Os-He isotopes in arsenopyrite. Geology 35, 795.

Ni, P., Wang, G.G., 2017. Multiple episodes of Cu-Au mineralization in the northeastern section of the QHMB induced by reworking of continental crust. Acta Petrol. Sin. 33, 3373–3394 in Chinese with English abstract.

Ni, P., Wang, G.G., Chen, H., Xu, Y.F., Guan, S.J., Pan, J.Y., Li, L., 2015. An Early Paleozoic orogenic gold belt along the Jiang-Shao Fault, South China: evidence from fluid inclusions and Rb-Sr dating of quartz in the Huangshan and Pingshui deposits. J. Asian Earth Sci. 103, 87–102.

Ohmoto, H., Goldhaber, M.B., 1997. Sulfur and carbon isotopes. In: Barnes, H.L. (Ed.), Geochemistry of Hydrothermal Ore Deposits, 3rd edn. Wiley, New York, pp. 517–611.

Ohmoto, H., Rye, R.O., 1979. Isotopes of sulfur and carbon. In: Barnes, H.L. (Ed.), Geochemistry of Hydrothermal Ore Deposits. John Wiley and Sons, New York, pp. 509–567.

Rollinson, H.R., 1993. Using Geochemical Data: Evaluation, Presentation, Interpretation. Longman Scientific and Technical Press, New York, pp. 1–352.

Shirey, S.B., Walker, R.J., 1998. The Re-Os isotope system in cosmochemistry and high-temperature geochemistry. Annu. Rev. Earth Pl. Sc. 26, 423–500.

Shu, L.S., 2006. Pre-Devonian tectonic evolution of south China: from Cathaysia Block to Caledonian folded belt. Geol. J. China Univ. 12, 418–431 in Chinese with English abstract.

Shu, L.S., 2012. An analysis of principal features of tectonic evolution in South China Block. Geol. Bull. China 31, 1035–1053 in Chinese with English abstract.

Smoliar, M.I., Walker, R.J., Morgan, J.W., 1996. Re–Os ages of group IIA, IIIA, IVA and IVB iron meteorites. Science 271, 1099–1102.

Soares, M.B., Selby, D., Robb, L., Neto, A.V.C., 2021. Sulfide recrystallization and gold remobilization during the 2.0 Ga stage of the Minas Orogeny: implications for gold mineralization in the Quadrilátero Ferrífero area. Brazil. Econ. Geol. 116, 1455–1466.

Thorpe, R.I., 1999. The Pb isotope linear array for volcanogenic massive sulfide deposits of the Abitibi and Wawa subprovinces, Canadian Shield. Economic Geology Monograph 10, 555–575.

Wang, G.G., Ni, P., Zhu, A.D., Wang, X.L., Li, L., Hu, J.S., Lin, W.H., Huang, B., 2018. 1.01–0.98 Ga mafic intra-plate magmatism and related Cu-Au mineralization in the eastern Jiangnan orogen: Evidence from Liujia and Tieshajie basalts. Precambr. Res. 309, 6–21.

Wang, J.Y., Santosh, M., Yang, C.X., Nakagawa, M., 2021. Revisiting the type area VMS deposit of Besshi, SW Japan: In-situ trace element chemistry, isotopes and Re-Os age of sulfides. Ore Geol. Rev. 130, 103955.

Xie, L., Wang, R.C., Chen, J., Zhu, J.C., 2010. Mineralogical evidence for magmatic and hydrothermal processes in the Qitianling oxidized tin-bearing granite (Hunan, South China): EMP and (MC)-LA-ICPMS investigations of three types of titanite. Chem. Geol. 276, 53–68.

Xu, Q.D., 1992. A discussion on the geology of Tieshajie copper polymetalogenic zone, Yiyang county, Jiangxi province. Geol. Jiangxi. 6, 374–379 in Chinese.

Ye, Q.T., 1987. Genetic and Ore-forming Series of Lead-Zinc Deposits in Northeast Jiangxi. Beijing Science and Technology Publishing House, Beijing, pp. 1–124 in Chinese.

Zhao, G., Cawood, P.A., 2012. Precambrian geology of China. Precambrian Res. 222–223, 13–54.

Zheng, S.X., 2020. Discussion on geological characteristics and genesis of silver ore in north Wuyi mountain area. China. Min. Mag. 29 (S1), 260–266 in Chinese with English abstract.

Zhou, Q., Jiang, Y.H., Zhao, P., Liao, S.Y., Jin, G.D., 2012. Origin of the Dexing Cu-bearing porphyries, SE China: elemental and Sr–Nd–Pb–Hf isotopic constraints. Int. Geol. Rev. 54, 572–592.

Zhou, Q., Jiang, Y.H., Zhang, H.H., Liao, S.Y., Jin, G.D., Zhao, P., Jia, R.Y., Liu, Z., 2013. Mantle origin of the Dexing porphyry copper deposit, SE China. Int. Geol. Rev. 55, 337–349.

Zhou, Y.Z., Li, X.Y., Zheng, Y., Shen, W.J., He, J.G., Yu, P.P., Niu, J., Zeng, C.Y., 2017. Geological settings and metallogenesis of Qinzhou Bay-Hangzhou Bay orogenic juncture belt, South China. Acta Petrol. Sin. 33, 667–681 in Chinese with English abstract.

Zhu, A.D., 2017. Genesis of the Tieshajie Cu -Pb-Zn-Ag Polymetallic Deposit, northeastern Jiangxi. Nanjing University. Master Dissertation (in Chinese with English abstract.